

Common Sense Bias Modeling for Classification Tasks

Miao Zhang¹ Zee Fryer² Ben Colman² Ali Shahriyari² Gaurav Bharaj²
¹New York University ²Reality Defender Inc

miaozhng@nyu.edu, {zee, ben, ali, gaurav}@realitydefender.ai

Abstract

Machine learning model bias can arise from dataset composition: correlated sensitive features can disturb the downstream classification model’s decision boundary and lead to performance differences along these features. Existing de-biasing works tackle most prominent bias features, like colors of digits or background of animals. However, a real-world dataset often includes a large number of feature correlations, that manifest intrinsically in the data as common sense information. Such spurious visual cues can further reduce model robustness. Thus, practitioners desire the whole picture of correlations and flexibility to treat concerned bias for specific domain tasks. With this goal, we propose a novel framework to extract comprehensive bias information in image datasets based on textual descriptions, a common sense-rich modality. Specifically, features are constructed by clustering noun phrase embeddings of similar semantics. Each feature’s appearance across a dataset is inferred and their co-occurrence statistics are measured, with spurious correlations optionally examined by a human-in-the-loop interface. Downstream experiments show that our method discovers novel model biases on multiple image benchmark datasets. Furthermore, the discovered bias can be mitigated by a simple data re-weighting strategy that de-correlates the features, and outperforms state-of-the-art unsupervised bias mitigation methods.

1. Introduction

Computer vision has been deployed with dramatically more diverse data (both realistic and generative) in recent years, which has drawn attention to data cleaning and bias reduction [40]. One common bias is due to the frequent co-occurrence of target features with context features (illustrated in Figure 1), that downstream task models may rely on to make predictions even though the relationship is not robust and generalizable [4, 37, 45].

Current unsupervised algorithms detect bias informed by model performance. For example, to separate samples aligning with and conflict to bias in model latent space

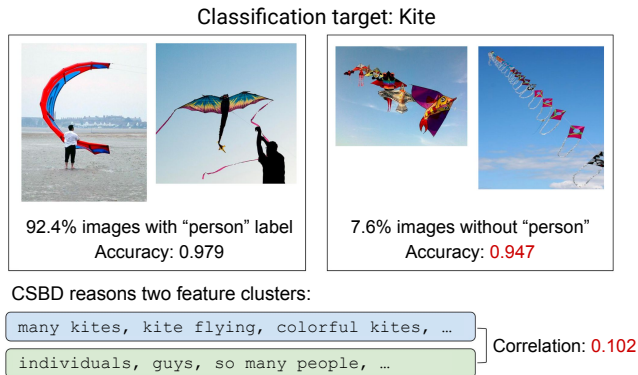


Figure 1. Spurious features are everywhere: Objects which co-occur frequently with the target can affect model prediction, for example, kites and people in MS-COCO. Spurious features like this are of multiple types and may cause different downstream biases. Our method aims to discover a comprehensive list of them based on common sense descriptions, and treat biases which have not been explored in literature.

[1, 14, 19, 36, 38], or by model gradient [1]. We observe that most approaches have only tackled limited bias types with prominent and delicate features, like the color of digits, the background of animals [28, 35], or the gender of the person doing certain activities [54]. It remains to be an open question whether more general image features, including those coarse and subtle ones in a dataset will correlate with the target feature in an *unwanted* way and affect model predictions. For example, small objects like a keyboard nearby a cat, a person nearby a kite which we discover to compose short-cut learning (Figure 1), have been overlooked for bias modeling.

These observations suggest to enrich bias signals, and we propose to model with additional data modalities, specifically text descriptions of images. Differentiating to labels, descriptions can cover a wider range of features that humans perceive (with respect to whole dataset instead of individual data samples as descriptions can be noisy). We show by experiments that debiasing based on supervision from description-derived bias obtains state-of-the-art results.

“Common sense reasoning” by natural language [3, 9, 15,

[32] is a popular approach for high-level abstract understanding of images and reasoning for subtle image features. There have been some early explorations in using this approach for bias discovery. For example, studies encode verbalized spurious features into text embeddings, then aligning to model latent space to measure feature influence [47, 52]. However, the use cases of the existing common sense bias modelings are restricted by the reliance on multi-modal models like CLIP [32] or generative models [34] to align embedding space of image and text. This additional step of alignment is challenging: it has a high requirements for representation quality and may not capture features from fine-grained image regions. There are also studies that analyze bias in dataset captions [41, 43], but their focus is on linguistic stereotypes within captions themselves, rather than using the captions to debias visual recognition.

To explore this direction, we design a novel description-based reasoning method for feature correlation and downstream model bias, called Common Sense Bias Discovery (CSBD). Given a description corpus of images (for example, captions), we unpack it into “features” through noun chunk clustering. These features are extracted from the semantic components of descriptions, which represent various image content, not limited by prior knowledge or cross-modal alignments. Then, correlations between features are quantified based on their co-occurrence across all data samples. It should note that discovered correlated features are not necessarily bias: for example, a correlation between “teeth” and “smile” in a dataset of face images is both expected and entirely benign. Therefore, we maintain a human-in-the-loop component to identify spurious correlations that should be addressed for specific tasks. However, following the identification step, our method does not require human intervention to mitigate the downstream model bias caused by these correlations. Our contributions are as follows:

1. A novel framework that uses textual descriptions obtained via humans or vision-language models that: (i) comprehensively analyzes spurious correlations contained in image datasets, and (ii) provides guidance on debiased downstream model training. Specifically:
2. A common sense reasoning approach that generates human interpretable “feature clusters”. Based on the discovered clusters, the formulations to derive pairwise correlations and re-sampling weights for model debiasing.
3. Experimental results show that our approach discovers biases with respect to static spurious features on multiple benchmarks, which to the best our knowledge have not been previously addressed. The resulting mitigation achieves state-of-the-art performances.

2. Related Work

Unsupervised bias discovery. Many recent studies have improved model robustness without requiring sensitive fea-

ture annotation. One approach is to assume that easy-to-learn data samples lead to shortcut feature learning, thus resulting in biased classifiers. These bias-aligning samples have higher prediction correctness and confidence [13, 17, 22, 51], larger gradient [1], or being fitted early in training [16, 28]. Feature clustering has also been used, which leverages the observation that samples with same the feature are located closely in model latent space. Bias is then identified based on the trained model’s unequal performance across clusters [14, 36]. Another approach finds bias related subgroups based on a certain amount of latent space directions that are highly correlated to model performance [53]. Most methods rely on additional biased learning to infer discounted samples, which might not be robust to shifts in training algorithm or schedules. Also, the implicit bias discovery used in these methods lacks transparency and interpretability. We propose a novel direction to discover dataset bias by description reasoning, which is agnostic and generalizable to different downstream learning schemes.

Bias mitigation. Methods that identify bias-conflicting samples or subgroups use them as supervision to upweight low performers, thus training a debiased model [1, 14, 16, 22, 28, 36, 53]. Alternatively, methods encourage models to learn similar representations for samples with the same target but different sensitive features via contrastive learning [29, 50, 51], e.g., augmenting bias-aligned images to alter sensitive features while maintaining the target content [13, 20, 33]. Bias mitigation method using regularization loss penalizes models for violations of the Equal Opportunity fairness criterion [19]. These frameworks address bias identified during model learning process and perform interventions accordingly. We approach the problem from a new perspective, recognizing that bias can take various forms captured by the common sense information of a dataset. Analyzing feature connections from this information can lead to simple and effective bias mitigation.

Bias discovery with human knowledge. Building machine learning systems with human judgement is crucial for user-centric and responsible goals [15, 44]. It enables domain expertise to be involved for improving real-world performances with minimal cost [48]. For bias discovery purposes, researchers have analyzed text-based item sets in visual question answering dataset and use association rules to interpret model behaviors [25]. Human is included to examine biases, including interpreting the semantic meaning of specific sensitive features [18] and analyzing bias information represented by the decomposition of sample subgroups in model latent space [53]. The studies motivate us for interpretable bias distillation. Image descriptions or captions are data formats rich of cognitive and common sense knowledge, thus are of great interests to be utilized for debiasing

supervision.

3. Method

As in Figure 2, we present our framework of discovering and treating bias supervised by image descriptions, **Common-Sense Bias Discovery** method, referred to as CSBD. In brief, given a corpus of (image, text description) pairs, our method generates clusters of noun chunks to indicate presence of features across samples. Then, pairwise feature¹ correlations are analyzed. This is followed by an optional human-in-the-loop module to allow a domain expert to review highly correlated features and select those that may negatively impact the downstream task. Finally, for any selected correlation to treat, we mitigate model bias via data re-weighting, without a requirement for sensitive group labels. Detailed algorithm steps are in the supplementary material. The three major components of the method are described in the following.

Language-inferred feature distribution. Natural language image descriptions must first be split into information units to align with image objects. We use the spaCy “en_core_web_sm” model [11] to extract noun chunks (noun and adjective grouped together), e.g. obtaining “The girl” and “a big smile” from “The girl has a big smile”, from all descriptions. We then use a general purpose sentence embedding model, the Universal Sentence Encoder [6], to map the noun chunks into high-dimensional vectors that represent their semantics, denoted as $\mathbf{A} \in \mathbb{R}^d$. The selection of this text embedding model is based on accuracy and computing speed. Next, we implement agglomerative clustering on \mathbf{A} . It starts from single vector as a cluster and hierarchically merges pairs of clusters until a certain criteria is reached, given no prior knowledge of the cluster number. We set the criteria to be the maximum Euclidean distance between any vectors of two clusters, denoted as z . It is a tunable hyper-parameter that controls the granularity of the clusters, e.g. “a boy” and “a young man” may be clustered together with a larger z and be in separate clusters with a smaller z . Each obtained cluster is viewed as a feature that is consistent with common sense descriptions.

Discovering feature correlations. Having extracted a set of feature clusters in the previous step, the next step is understanding feature co-occurrence within the dataset. This allows us to identify spurious correlations relevant to the target task, which may cause model bias. To quantify such correlations: first, we generate a binary indicator for whether each feature is present: $\mathbf{t}_f = [t_1, t_2, \dots, t_N]$, where N is the size of the dataset, and $t_i = 1$ if feature f occurs in the i^{th} image’s description, otherwise $t_i = 0$. Second, the phi coefficient ϕ [8, p. 282]² is used to measure the association

¹“Feature” in this work refers to a cluster of semantically similar phrases, e.g. “beaming smile” and “wide smile” are considered interchangeable and belong to one cluster/feature.

²Also known as the Matthews correlation coefficient [26].

between every two feature indicators. The ϕ between two indicators \mathbf{t}_f and $\mathbf{t}_{f'}$ is defined as follows:

$$\phi_{\mathbf{t}_f \mathbf{t}_{f'}} = \frac{x_{11}x_{00} - x_{10}x_{01}}{\sqrt{x_{1*}x_{0*}x_{*0}x_{*1}}}, \quad (1)$$

where $c \in [0, C)$, $f, f' \in [0, F_c]$, and

$$\begin{aligned} x_{11} &= \|\mathbf{t}_f \cdot \mathbf{t}_{f'}\|_1, & x_{01} &= \|(-\mathbf{t}_f) \cdot \mathbf{t}_{f'}\|_1, \\ x_{10} &= \|\mathbf{t}_f \cdot (-\mathbf{t}_{f'})\|_1, & x_{00} &= \|(-\mathbf{t}_f) \cdot (-\mathbf{t}_{f'})\|_1, \\ x_{1*} &= \|\mathbf{t}_f\|_1, & x_{0*} &= \|-\mathbf{t}_f\|_1, \\ x_{*0} &= \|-\mathbf{t}_{f'}\|_1, & x_{*1} &= \|\mathbf{t}_{f'}\|_1. \end{aligned}$$

\neg denotes element-wise negation, $\|\cdot\|_1$ denotes the L^1 norm.

Two features are positively correlated (likely to co-occur in an image) if ϕ is a positive value, and are negatively correlated (rarely co-occur) if ϕ is a negative value. A ϕ near zero indicates two features which co-occur randomly. Intuitively, features that have high correlation with any target features can become shortcuts for model learning and cause biased decision-making toward certain subgroups [5, 39]. Thus, feature pairs sorted by ϕ are returned for examination by humans, who have access to the common sense text description of each feature.

Strength of human evaluated bias. In many cases, the extracted feature pairs are naturally connected (e.g. “teeth visible” with “a smile”, and most facial features with “the face”). These correlations are usually robust and generalizable, and thus viewed as benign. The benign correlations usually exist, besides, the function of correlations vary across different downstream learning scenarios and not all correlations need to be treated. Therefore, a human-in-the-loop step is necessary to ensure that only spurious correlations that may impact the target task are selected. The human-in-the-loop component of our pipeline, like previous efforts [18, 25, 47, 52], allows flexibility and transparency for bias mitigation. The human involvement is *optional*, that if given any bias features blindly, our method will generate the mitigation approach as described below.

Bias mitigation via re-weighting. We use the feature correlation signals inferred from textual descriptions to mitigate vision model bias. Since adjusting sampling weights to intervene model learning for discounted samples is a frequently used approach [1, 36, 46], and our goal is *not* to design novel sampling strategies, we use a state-of-the-art sampling method [31] based on our analyzed feature presence (\mathbf{t}). We compute data sampling weights (or probabilities) with the goal to de-correlate the presence of the spurious feature³ and the target feature. Specifically, We denote the dataset

³We use the term “spurious features” to reflect the fact that the primary biases of interest in literature often relate to features such as race/gender/disability/sexuality/etc; however, as we see in Table 2, our method is flexible enough to capture more unexpected types of unwarranted correlation, e.g. “cat” and “couch”.

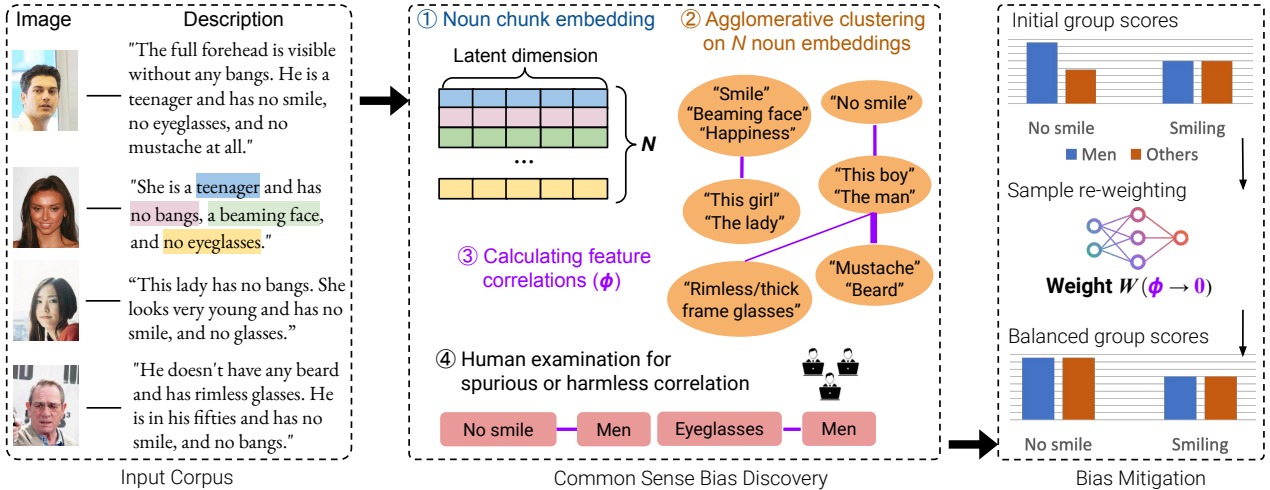


Figure 2. *Common Sense Bias Discovery (CSBD) system and the mitigation strategy overview*: (Left) Input corpus of image and corresponding description pairs are given. (Middle) (1) Descriptions are split into semantically meaningful noun chunks and encoded into representation vectors. (2) A hierarchical clustering on the vector set generates a list of common sense feature clusters. (3) Correlations between the presence of every two features are computed. (4) Highly-correlated features are examined by a human for mitigation. (Right) Finally, correlations are mitigated by adjusting image sampling weights during model training, automatically calculated from the derived feature presence statistics.

as D , the target feature indicator as t_y , the spurious feature indicator as t_s , and the conditional probability of t_s given t_y as $P_D(t_s|t_y)$. The new sampling probability for each element in D ensures that feature s is present in the same probability regardless of whether feature y is present or not:

$$P'_D(t_s = 1|t_y = 0) = P'_D(t_s = 1|t_y = 1) \quad (2)$$

This equation ensures independence between s and y across the dataset [31]. Additionally, we implement randomized augmentations alongside the sampling weights to enhance data diversity.

4. Experiments

4.1. Datasets

CelebA-Dialog [12] is a visual-language dataset including captions for images in CelebA [24], a popular face recognition benchmark dataset containing 40 facial attributes. Each caption describes 5 labels: “Bangs”, “Eyeglasses”, “Beard”, “Smiling”, and “Age”. The benefit of captions in natural language is that they also include other common sense information like pronouns and people titles (phrases like “the man” or “the lady”). We identify feature correlations for this dataset accordingly (see Figure 3). For classification tasks, we select different target labels to recognize and spurious feature labels to evaluate bias results (here “label” refers to the ground truth binary labels used only for evaluation). The labels are selected because their corresponding caption-

inferred features are discovered by our method to be highly correlated and thus may cause downstream model bias.

MS-COCO 2014 [21] is a large-scale scene image datasets including annotations for 80 objects, and each image has 5 descriptive captions generated independently [7]. We randomly select 1 caption for each image. Based on our feature correlation analysis, we select 9 target and spurious feature pairs for training downstream models and evaluating bias, as listed in Table 2. For example, we train a model for recognizing “Dog” and evaluate if the model shows performance disparity for images with/without “Frisbee”. We perform binary classification on each target label, following [42]. This is because although MS-COCO is more used for multi-label classification, certain labels will need to be treated as auxiliary features in order to reveal their influence on the target thus study bias caused by feature correlations.

LVM-generated caption. We also apply our proposed method to image captions generated using large vision language model (LVM). This data source is considered since human annotated caption is not always available and is especially expensive on large scale datasets. We use the open-source LLaVA-Next 7B parameter model [23] to caption images of CelebA dataset with prompt “Please describe face attributes in this image”, and MS-COCO dataset with prompt “Please describe the scene in this image”. We evaluate captioning quality of the model on MS-COCO against five ground

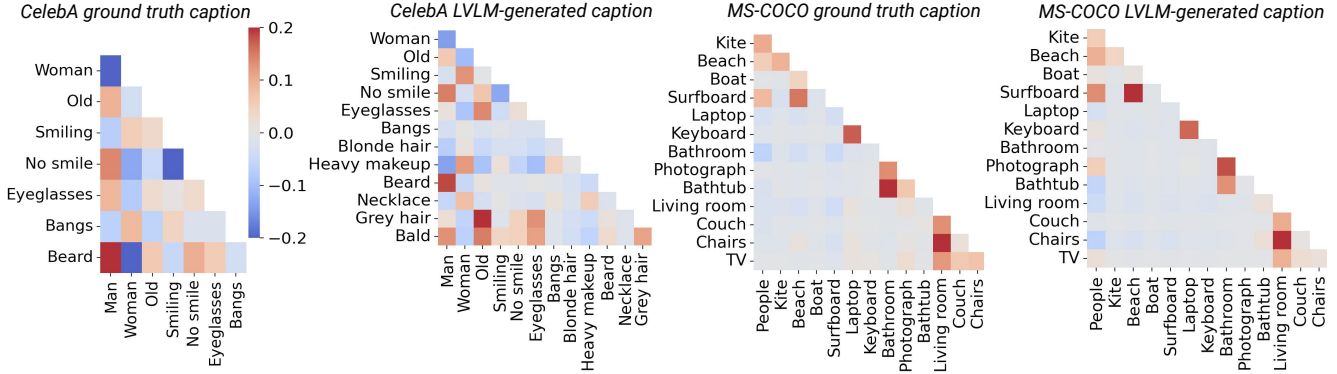


Figure 3. Part of correlated features and their correlation coefficients analyzed by CSBD on CelebA and MS-COCO datasets. Two types of common sense descriptions are used: human-generated (ground truth) and LVLM-generated caption.

truth captions. The SPICE [2] metric on the validation set has an average score of 0.1583, showing a satisfying ability of the LVLM model to capture image features and their relations. Besides, we evaluate the common sense biases modeled from LVLM-generated caption when applying our proposed method, which is in general consistent with the results obtained with ground truth captions (Figure 3).

4.2. Implementation

For correlation reasoning, the noun chunks from the description corpus are encoded as vectors in 512 dimensions using the Universal Sentence Encoder. Dimension reduction is performed using PCA before clustering, ensuring that the sum of the PCA components accounts for a high amount of variance ($>90\%$). The distance criterion for generating feature clusters is set to $z = 1.0$; see ablation sections for sensitivity analysis. We use Chi-square test [30] to verify significance of derived correlation coefficients.

For the downstream training, we use the same training, validation, and testing split as in [51] for CelebA dataset, and as in [27] for MS-COCO dataset. However, because of label scarcity of individual objects relative to the entire dataset (for example, only 3% of images in MS-COCO contain “Cat” and 2% of images contain “Kite”), to avoid class imbalance problem introducing confounding bias to the classifier, we randomly take subsets of the dataset splits which include 50% of each target label. Experiments are based on three independent runs which provide the mean and standard deviation results.

4.3. Results

Bias discovery and mitigation are both needed for reliable model training. While the emphasis of the proposed method is to analyze bias from datasets, not primarily on mitigation algorithm, it is important to verify on downstream tasks that the method “discovers” correlations in the dataset that the model actually takes a shortcut for learning. So in this

section, we first present bias discovery results on the two benchmark datasets. Then, we analyze robustness of the correlation derivation, with respect to potential errors and incompleteness of descriptions. Finally, we perform thorough downstream evaluations to show that reducing feature dependence analyzed by the proposed method serves as a practical and effective debiasing objective.

4.3.1 Correlation discovery results

Figure 3 presents selected correlated feature pairs for CelebA and MS-COCO dataset. It shows that both human-annotated and LVLM-generated captions contain rich common sense information that can be distilled into distinctive features. The correlation between the obtained features are consistent across different image descriptions, highlighting the description-agnostic and generalization strength of the proposed method. We note that Figure 3 shows limited CelebA feature correlations with the ground truth caption because the caption is designed to annotate only five features.

The description-derived features include those not represented in the dataset labels and reveal highly correlated ones, such as “city street” and “bus”. The spuriously correlated features are frequently seen but not generalizable to all samples, so models cannot predict one feature robustly if relying on the other: for example, recognition of a bus in an image might depend not on its appearance but on whether the background is a city street. On CelebA dataset, facial features “smiling”, “eyeglasses”, “bangs”, etc, are spuriously correlated to gender features “man”, “woman”, and age features “young”, etc. Other strong correlations include “Receding hairline” and “grey hair” which aligns with common sense but lacks robustness. We designate naturally related features like “mouth” and “smiling” as benign. On MS-COCO dataset, benign correlations include “frisbee” and “a game”, “waves” and “ocean”, etc. The spurious ones include “cat”

Target	Spurious	No mitigation		LfF		DebiAN		PGD		BPA		CSBD (ours)	
		Wst. (↑)	Avg. (↑)	Wst.	Avg.	Wst.	Avg.	Wst.	Avg.	Wst.	Avg.	Wst.	Avg.
Smiling	Male	0.894	0.919	0.730	0.841	0.895	0.916	0.888	0.917	<u>0.899</u>	0.912	0.908	<u>0.918</u>
Eyeglasses	Male	0.962	<u>0.986</u>	0.912	0.963	0.967	0.979	0.966	0.984	<u>0.971</u>	0.983	0.973	0.987
Young *	Eyeglasses *	<u>0.652</u>	<u>0.818</u>	0.640	0.805	0.609	0.796	0.646	0.817	0.638	0.806	0.655	0.820
Receding hairline *	Grey hair *	0.186	0.650	0.174	0.648	0.198	0.680	0.225	0.672	0.351	0.521	<u>0.337</u>	0.680

Table 1. Treating common sense bias towards the target label (Target) among the spurious feature label (Spurious) on CelebA. The starred labels (*) represent that CSBD uses LVM-generated descriptions to discover and mitigate bias. The metric for debiasing effectiveness: the worst performing group (Wst.), and average accuracy of all target-spurious feature groups (Avg.), are reported. The best results are in bold and the second best results are underlined.

Target	Spurious	No mitigation		LfF		DebiAN		PGD		BPA		CSBD (ours)	
		Wst.(↑)	Avg. (↑)	Wst.	Avg.	Wst.	Avg.	Wst.	Avg.	Wst.	Avg.	Wst.	Avg.
Cat	Couch	0.849	0.935	0.800	0.916	0.821	0.902	<u>0.884</u>	<u>0.940</u>	0.853	0.925	0.906	0.941
Cat	Keyboard	<u>0.948</u>	0.972	0.870	0.938	0.917	0.949	0.947	0.977	0.890	0.952	0.953	<u>0.976</u>
Dog	Frisbee	<u>0.883</u>	0.927	0.821	0.893	0.845	0.872	0.940	0.854	0.905	0.905	0.903	<u>0.934</u>
TV	Chair	0.726	0.893	0.690	0.867	0.718	0.876	<u>0.821</u>	<u>0.907</u>	0.758	0.887	0.842	0.911
Umbrella	Person	0.761	0.880	0.771	0.854	0.716	0.857	<u>0.763</u>	<u>0.887</u>	<u>0.777</u>	0.878	0.814	0.892
Kite	Person	0.937	0.963	0.854	0.923	<u>0.941</u>	<u>0.960</u>	0.917	0.955	0.921	0.957	0.945	<u>0.960</u>
Wine glasses *	Person *	<u>0.848</u>	0.888	0.834	0.869	0.838	0.873	0.828	0.869	0.844	<u>0.890</u>	0.860	0.894
Pizza *	Oven *	0.828	0.916	0.820	0.861	0.827	0.910	0.828	0.903	<u>0.854</u>	<u>0.925</u>	0.862	0.932

Table 2. Treating part of the discovered biases for binary object classification task on MS-COCO dataset.

and “couch”, “kite” and “people”, “bathroom” and “photograph”, etc. The full list of correlated feature pairs and their coefficient values are in the Supplementary.

4.3.2 Correlation robustness evaluation

First, we test the robustness of analyzed feature presence, considering that unlike dataset label, description annotators may only select features relevant or noticeable to them, causing incompleteness or faults. Indeed, prior studies [43, 49] have highlighted the incorrect and low-quality captions in MS-COCO. We randomly select 20 common sense features derived from MS-COCO captions and compare them with their corresponding labels. We compute the Pearson correlation coefficient between the presence of each feature and label across the dataset, obtaining a coefficient of 0.545 (95% confidence interval 0.153 to 0.937). This indicates a moderate correlation between label and feature distribution, which varies across different features. The inconsistency between common sense feature and label distribution is expected, influenced by both caption quality (captions may incorrectly describe ground truth label) and text embedding clustering (text with similar semantics may not be encoded closely in the representation space).

Next, we test the robustness of discovered feature correlations (or bias, to avoid confusion with the correlation

test here, we use the term “bias”) under this circumstance. Bias existence between each feature and each of the remaining features is computed. The same bias measurement is then performed using labels. The correlation coefficient between the two measurements is 0.781 (95% confidence interval 0.417 to 1.0), which is much higher and shows lower variance than the result for feature presence. The analysis indicates that the proposed method operates not at the level of individual images but rather at the dataset level to identify trends in correlations, thus showing certain robustness to noise and incompleteness present in image descriptions.

4.3.3 Bias mitigation results

Spurious feature correlations discovered by CSBD can indicate and help mitigate downstream model bias, as shown by image classification results on CelebA and MS-COCO dataset in Table 1 and Table 2. We use the worst group performance (Wst.) to evaluate model bias, and average group performance (Avg.) to evaluate model quality, following [1, 36, 51]. The groups here are all combinations of target label and spurious feature label pairs as in [51]. The comparison baselines are unsupervised bias mitigation methods. They include LfF [28] which upweights failure samples, DebiAN [19] which uses additional bias predictor, and re-sampling methods PGD [1] based on sample gradients, and

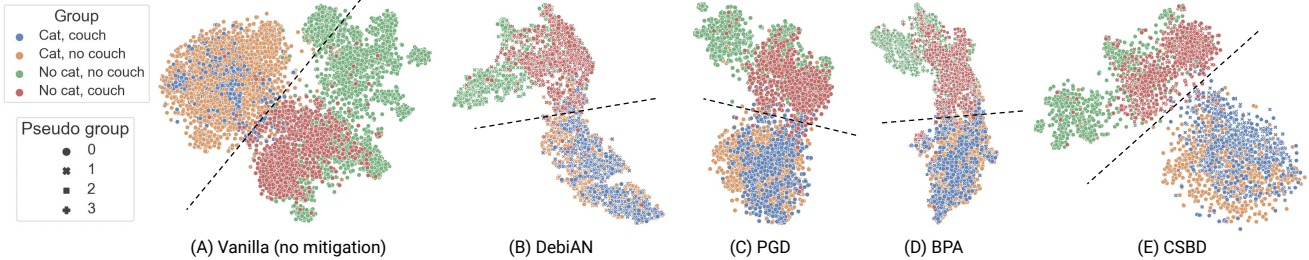


Figure 4. T-SNE results for sample embeddings of cat classifiers (“Couch” as sensitive label) trained with MS-COCO. Target label: “Cat” (blue & orange) and “No cat” (green & red) are most linearly separable (model decision boundary is indicated by the dotted straight line) with CSBD compared to other baselines. For bias discovery, methods are marked with their assigned bias-aligning and bias-conflict samples (Pseudo group). Only CSBD discovers thus treats the sensitive feature couch (E).

BPA based on latent space clusters [36].

Baseline model without bias mitigation presents a gap between Wst. and Avg. for all tasks, indicating model biases that align with our reasoning on the datasets. For example, images containing chair but no TV obtain an accuracy of 0.726 for TV classification, 19% lower than the average accuracy. Face images to recognize receding hairline with dark hair show an accuracy of 0.186, while the recognition with grey hair has an accuracy over 0.99 because of strong correlation between these two features. CSBD successfully mitigates model bias (most improved Wst.) on all targets, outperforming the baseline with no mitigation and other debiasing methods. Importantly, model classification quality is not degraded by using our method: CSBD always obtains the highest or the second Avg. Bias mitigation based on LVLMM generated descriptions are effective on both datasets, which shows our method’s generalizability to different description corpus and wide applicability to bias mitigation problems.

5. Discussion

We investigate the advantage of our method for bias mitigation by checking how well they separate target objects not affected by spurious features in latent space. We visualize image embeddings extracted from the last fully connected layer of the “Cat” classifier trained with MS-COCO. Model bias can be observed from the baseline (no mitigation) (Figure 4 (A)): while the “Cat” targets are separable for samples without the spurious feature “Couch”, for images *with* the spurious feature, the model prediction boundary for the targets is blurred (blue and red dots are partially mixed).

The same embedding analysis is performed for bias mitigation methods⁴. As shown in Figure 4 (B-D), DebiAN, PGD, and BPA do not fix model’s biased decision rule, that the model cannot distinguish two targets (“Cat” and ‘No cat’ samples), indicated by the dotted straight line. Instead, the methods only mix samples within a target class more closely. The reason is that the methods identify discrepancy between

sample representations or gradients as bias and try to mitigate the discrepancy. However, the detected discrepancy fails to accurately capture the unwanted feature responsible for mis-classifying bias-conflicting samples (those near the decision boundary), so the black-box way of mitigation proves less effective for de-biasing.

z	0.5	0.8	0.9	1	1.2	1.5
ϕ	0.0608	0.0608	0.0908	0.0908	0.107	0.175
Wst. (\uparrow)	0.971	0.972	0.973	0.973	0.973	0.972
Avg. (\uparrow)	0.986	0.986	0.986	0.987	0.987	0.986

Table 3. Sensitivity analysis on the distance threshold z used for splitting feature clusters. z within a reasonable range can discover consistent correlated features ($\phi > 0$) and produce similar bias mitigation results (Wst.), between “eyeglasses” and “man” features on CelebA.

Ablation on the clustering threshold Feature clusters are obtained by agglomerative clustering on noun chunk embeddings so that the complete linkage between two clusters is lower than a hyper-parameter z . This tune-able parameter affects the granularity of discovered feature clusters and whether reasonable bias can be derived. As shown in Table 3, the bias mitigation (Wst.) and classification (Avg.) results are robust to different z , which indicates that feature clusters and their distributions are captured precisely in all cases. The granularity and content of feature clusters change with different z , which result in different correlation coefficient ϕ . Here, “eyeglasses” and “sunglasses” are one feature with $z = \{1.2, 1.5\}$ and shows a stronger correlation to “man” feature, but they are separate features with smaller z and “eyeglasses” alone shows weaker correlation to “man”. The selection of z should be tuned based on the granularity of features that practitioners hope to derive and find biases with. For example, if z is too large (we test with $z = 5$), gender clusters will be replaced by a

⁴Here only showing methods outperforming no mitigation.

“people” cluster, thus the bias: man wearing glasses more will not be discovered on the CelebA dataset.

Ablation on re-sampling weights. We ablate the bias mitigation step by skewing the sampling weights W analyzed by CSBD. Specifically, for any images that need to be over-sampled ($W[i] = 1 + p$ for the i^{th} sample), we first double their increased weight by $W[i] = 1 + 2 * p$. The same downstream task to classify “Cat” with spurious attribute “Couch” on MS-COCO is performed. The model obtains Wst.: 0.904, Avg.: 0.940. Then, we only use half of the increased weight by $W[i] = 1 + 0.5 * p$, and the model obtains Wst.: 0.881, Avg.: 0.936. Compared to the results in Table 2, though training with skewed weights still outperforms the vanilla setting with no intervention, the bias mitigation and accuracy results are slightly discounted. It shows that the data re-sampling weights computed from CSBD is the key for effective bias mitigation.

6. Conclusion and Limitation

This work proposes to use textural descriptions of a dataset for systematic bias discovery and mitigation. The approach leads to a new perspective on bias problems regarding how we can use knowledge in natural language to precisely reduce a concerned feature’s influence to image classification tasks. Our algorithm applies common sense reasoning to descriptions, which cover a wide range of image features not annotated by the label set, and indicates how feature correlations to the target will cause downstream bias. Experiment results show novel spurious correlations and model biases discovered for two vision benchmark datasets, and the state-of-the-art bias mitigation based on the discovery.

Limitations and future work. Though our method can model correlations between features beyond the labeled cohort, the discovered biases are limited to features included in textual descriptions. Besides, there are multiple topics to continue in this direction: First, we only study pairwise feature correlations, but higher degrees of correlations and how they affect model performance could be explored. Second, our method has not yet been tested in other vision recognition tasks and models, such as object detection and segmentation. However, since the method for discovering spurious feature correlations is agnostic to downstream tasks, this can be a direct next step.

References

- [1] Sumyeong Ahn, Seongyeon Kim, and Se-young Yun. Mitigating dataset bias by using per-sample gradient. In *Eleventh International Conference on Learning Representations*. ICLR, 2023. 1, 2, 3, 6
- [2] Peter Anderson, Basura Fernando, Mark Johnson, and Stephen Gould. Spice: Semantic propositional image caption evaluation. In *ECCV*, 2016. 5
- [3] Stanislaw Antol, Aishwarya Agrawal, Jiasen Lu, Margaret Mitchell, Dhruv Batra, C Lawrence Zitnick, and Devi Parikh. Vqa: Visual question answering. In *Proceedings of the IEEE international conference on computer vision*, pages 2425–2433, 2015. 1
- [4] Abhisha Basu, R Venkatesh Babu, and Danish Pruthi. Inspecting the geographical representativeness of images from text-to-image models. *arXiv preprint arXiv:2305.11080*, 2023. 1
- [5] Alexander Brown, Nenad Tomasev, Jan Freyberg, Yuan Liu, Alan Karthikesalingam, and Jessica Schrouff. Detecting shortcut learning for fair medical ai using shortcut testing. *Nature Communications*, 14(1):4314, 2023. 3
- [6] Daniel Cer, Yinfei Yang, Sheng-yi Kong, Nan Hua, Nicole Limtiaco, Rhomni St John, Noah Constant, Mario Guajardo-Cespedes, Steve Yuan, Chris Tar, et al. Universal sentence encoder. *arXiv preprint arXiv:1803.11175*, 2018. 3
- [7] Xinlei Chen, Hao Fang, Tsung-Yi Lin, Ramakrishna Vedantam, Saurabh Gupta, Piotr Dollár, and C Lawrence Zitnick. Microsoft coco captions: Data collection and evaluation server. *arXiv preprint arXiv:1504.00325*, 2015. 4
- [8] Harald Cramér. *Mathematical methods of statistics*. 1946. 3
- [9] Markos Diomataris, Nikolaos Gkanatsios, Vassilis Pitsikalis, and Petros Maragos. Grounding consistency: Distilling spatial common sense for precise visual relationship detection. In *Proceedings of the IEEE/CVF International Conference on Computer Vision*, pages 15911–15920, 2021. 1
- [10] Kaiming He, Xiangyu Zhang, Shaoqing Ren, and Jian Sun. Deep residual learning for image recognition. In *Proceedings of the IEEE conference on computer vision and pattern recognition*, pages 770–778, 2016. 1
- [11] Matthew Honnibal and Ines Montani. spacy 2: Natural language understanding with bloom embeddings, convolutional neural networks and incremental parsing. *To appear*, 7(1): 411–420, 2017. 3
- [12] Yuming Jiang, Ziqi Huang, Xingang Pan, Chen Change Loy, and Ziwei Liu. Talk-to-edit: Fine-grained facial editing via dialog. In *Proceedings of the IEEE/CVF International Conference on Computer Vision*, pages 13799–13808, 2021. 4
- [13] Eungyeup Kim, Jihyeon Lee, and Jaegul Choo. Biaswap: Removing dataset bias with bias-tailored swapping augmentation. In *Proceedings of the IEEE/CVF International Conference on Computer Vision*, pages 14992–15001, 2021. 2
- [14] Arvindkumar Krishnakumar, Viraj Prabhu, Sruthi Sudhakar, and Judy Hoffman. Udis: Unsupervised discovery of bias in deep visual recognition models. In *British Machine Vision Conference (BMVC)*, page 3, 2021. 1, 2
- [15] Brenden M Lake, Tomer D Ullman, Joshua B Tenenbaum, and Samuel J Gershman. Building machines that learn and think like people. *Behavioral and brain sciences*, 40:e253, 2017. 1, 2
- [16] Jungsoo Lee, Jeonghoon Park, Daeyoung Kim, Juyoung Lee, Edward Choi, and Jaegul Choo. Revisiting the importance of amplifying bias for debiasing. In *Proceedings of the AAAI Conference on Artificial Intelligence*, pages 14974–14981, 2023. 2
- [17] Jiaxuan Li, Duc Minh Vo, and Hideki Nakayama. Partition-and-debias: Agnostic biases mitigation via a mixture of

- biases-specific experts. In *Proceedings of the IEEE/CVF International Conference on Computer Vision*, pages 4924–4934, 2023. 2
- [18] Zhiheng Li and Chenliang Xu. Discover the unknown biased attribute of an image classifier. In *Proceedings of the IEEE/CVF International Conference on Computer Vision*, pages 14970–14979, 2021. 2, 3
- [19] Zhiheng Li, Anthony Hoogs, and Chenliang Xu. Discover and mitigate unknown biases with debiasing alternate networks. In *European Conference on Computer Vision*, pages 270–288. Springer, 2022. 1, 2, 6
- [20] Jongin Lim, Youngdong Kim, Byungjai Kim, Chanho Ahn, Jinwoo Shin, Eunho Yang, and Seungju Han. Biasadv: Bias-adversarial augmentation for model debiasing. In *Proceedings of the IEEE/CVF conference on computer vision and pattern recognition*, pages 3832–3841, 2023. 2
- [21] Tsung-Yi Lin, Michael Maire, Serge Belongie, James Hays, Pietro Perona, Deva Ramanan, Piotr Dollár, and C Lawrence Zitnick. Microsoft coco: Common objects in context. In *Computer Vision—ECCV 2014: 13th European Conference, Zurich, Switzerland, September 6–12, 2014, Proceedings, Part V 13*, pages 740–755. Springer, 2014. 4
- [22] Evan Z Liu, Behzad Haghgoo, Annie S Chen, Aditi Raghunathan, Pang Wei Koh, Shiori Sagawa, Percy Liang, and Chelsea Finn. Just train twice: Improving group robustness without training group information. In *International Conference on Machine Learning*, pages 6781–6792. PMLR, 2021. 2
- [23] Haotian Liu, Chunyuan Li, Yuheng Li, Bo Li, Yuanhan Zhang, Sheng Shen, and Yong Jae Lee. Llava-next: Improved reasoning, ocr, and world knowledge, 2024. 4
- [24] Ziwei Liu, Ping Luo, Xiaogang Wang, and Xiaoou Tang. Deep learning face attributes in the wild. In *Proceedings of the IEEE international conference on computer vision*, pages 3730–3738, 2015. 4
- [25] Varun Manjunatha, Nirat Saini, and Larry S Davis. Explicit bias discovery in visual question answering models. In *Proceedings of the IEEE/CVF Conference on Computer Vision and Pattern Recognition*, pages 9562–9571, 2019. 2, 3
- [26] Brian W. Matthews. Comparison of the predicted and observed secondary structure of t4 phage lysozyme. *Biochimica et biophysica acta*, 405 2:442–51, 1975. 3
- [27] Ishan Misra, C Lawrence Zitnick, Margaret Mitchell, and Ross Girshick. Seeing through the human reporting bias: Visual classifiers from noisy human-centric labels. In *Proceedings of the IEEE conference on computer vision and pattern recognition*, pages 2930–2939, 2016. 5
- [28] Junhyun Nam, Hyuntak Cha, Sungsoo Ahn, Jaeho Lee, and Jinwoo Shin. Learning from failure: De-biasing classifier from biased classifier. *Advances in Neural Information Processing Systems*, 33:20673–20684, 2020. 1, 2, 6
- [29] Sungho Park, Jewook Lee, Pilhyeon Lee, Sunhee Hwang, Dohyung Kim, and Hyeran Byun. Fair contrastive learning for facial attribute classification. In *Proceedings of the IEEE/CVF Conference on Computer Vision and Pattern Recognition*, pages 10389–10398, 2022. 2
- [30] Karl Pearson. X. on the criterion that a given system of deviations from the probable in the case of a correlated system of variables is such that it can be reasonably supposed to have arisen from random sampling. *The London, Edinburgh, and Dublin Philosophical Magazine and Journal of Science*, 50 (302):157–175, 1900. 5
- [31] Maan Qraitem, Kate Saenko, and Bryan A Plummer. Bias mimicking: A simple sampling approach for bias mitigation. In *Proceedings of the IEEE/CVF Conference on Computer Vision and Pattern Recognition*, pages 20311–20320, 2023. 3, 4
- [32] Alec Radford, Jong Wook Kim, Chris Hallacy, Aditya Ramesh, Gabriel Goh, Sandhini Agarwal, Girish Sastry, Amanda Askell, Pamela Mishkin, Jack Clark, et al. Learning transferable visual models from natural language supervision. In *International conference on machine learning*, pages 8748–8763. PMLR, 2021. 2
- [33] Vikram V Ramaswamy, Sunnie SY Kim, and Olga Russakovsky. Fair attribute classification through latent space de-biasing. In *Proceedings of the IEEE/CVF conference on computer vision and pattern recognition*, pages 9301–9310, 2021. 2
- [34] Robin Rombach, Andreas Blattmann, Dominik Lorenz, Patrick Esser, and Björn Ommer. High-resolution image synthesis with latent diffusion models. In *Proceedings of the IEEE/CVF conference on computer vision and pattern recognition*, pages 10684–10695, 2022. 2
- [35] Shiori Sagawa, Pang Wei Koh, Tatsunori B Hashimoto, and Percy Liang. Distributionally robust neural networks for group shifts: On the importance of regularization for worst-case generalization. *arXiv preprint arXiv:1911.08731*, 2019. 1
- [36] Seonguk Seo, Joon-Young Lee, and Bohyung Han. Unsupervised learning of debiased representations with pseudo-attributes. In *Proceedings of the IEEE/CVF Conference on Computer Vision and Pattern Recognition*, pages 16742–16751, 2022. 1, 2, 3, 6, 7
- [37] Krishna Kumar Singh, Dhruv Mahajan, Kristen Grauman, Yong Jae Lee, Matt Feiszli, and Deepti Ghadiyaram. Don’t judge an object by its context: Learning to overcome contextual bias. In *Proceedings of the IEEE/CVF Conference on Computer Vision and Pattern Recognition*, pages 11070–11078, 2020. 1
- [38] Nimit Sohoni, Jared Dunnmon, Geoffrey Angus, Albert Gu, and Christopher Ré. No subclass left behind: Fine-grained robustness in coarse-grained classification problems. *Advances in Neural Information Processing Systems*, 33:19339–19352, 2020. 1
- [39] Huan Tian, Tianqing Zhu, Wei Liu, and Wanlei Zhou. Image fairness in deep learning: problems, models, and challenges. *Neural Computing and Applications*, 34(15):12875–12893, 2022. 3
- [40] Antonio Torralba and Alexei A Efros. Unbiased look at dataset bias. In *CVPR 2011*, pages 1521–1528. IEEE, 2011. 1
- [41] Emiel Van Miltenburg. Stereotyping and bias in the flickr30k dataset. *arXiv preprint arXiv:1605.06083*, 2016. 2
- [42] Angelina Wang and Olga Russakovsky. Overwriting pre-trained bias with finetuning data. In *Proceedings of the*

- IEEE/CVF International Conference on Computer Vision*, pages 3957–3968, 2023. 4
- [43] Angelina Wang, Solon Barocas, Kristen Laird, and Hanna Wallach. Measuring representational harms in image captioning. In *Proceedings of the 2022 ACM Conference on Fairness, Accountability, and Transparency*, pages 324–335, 2022. 2, 6
- [44] Danding Wang, Qian Yang, Ashraf Abdul, and Brian Y Lim. Designing theory-driven user-centric explainable ai. In *Proceedings of the 2019 CHI conference on human factors in computing systems*, pages 1–15, 2019. 2
- [45] Yining Wang, Junjie Sun, Chenyue Wang, Mi Zhang, and Min Yang. Navigate beyond shortcuts: Debaised learning through the lens of neural collapse. In *Proceedings of the IEEE/CVF Conference on Computer Vision and Pattern Recognition*, pages 12322–12331, 2024. 1
- [46] Zeyu Wang, Klint Qinami, Ioannis Christos Karakozis, Kyle Genova, Prem Nair, Kenji Hata, and Olga Russakovsky. Towards fairness in visual recognition: Effective strategies for bias mitigation. In *Proceedings of the IEEE/CVF conference on computer vision and pattern recognition*, pages 8919–8928, 2020. 3
- [47] Shirley Wu, Mert Yuksekgonul, Linjun Zhang, and James Zou. Discover and cure: Concept-aware mitigation of spurious correlation. *arXiv preprint arXiv:2305.00650*, 2023. 2, 3
- [48] Xingjiao Wu, Luwei Xiao, Yixuan Sun, Junhang Zhang, Tianlong Ma, and Liang He. A survey of human-in-the-loop for machine learning. *Future Generation Computer Systems*, 135: 364–381, 2022. 2
- [49] Boxi Yu, Zhiqing Zhong, Xinran Qin, Jiayi Yao, Yuancheng Wang, and Pinjia He. Automated testing of image captioning systems. In *Proceedings of the 31st ACM SIGSOFT International Symposium on Software Testing and Analysis*, pages 467–479, 2022. 6
- [50] Fengda Zhang, Kun Kuang, Long Chen, Yuxuan Liu, Chao Wu, and Jun Xiao. Fairness-aware contrastive learning with partially annotated sensitive attributes. In *The Eleventh International Conference on Learning Representations*, 2022. 2
- [51] Michael Zhang, Nimit S Sohoni, Hongyang R Zhang, Chelsea Finn, and Christopher Ré. Correct-n-contrast: A contrastive approach for improving robustness to spurious correlations. *arXiv preprint arXiv:2203.01517*, 2022. 2, 5, 6
- [52] Yuhui Zhang, Jeff Z HaoChen, Shih-Cheng Huang, Kuan-Chieh Wang, James Zou, and Serena Yeung. Diagnosing and rectifying vision models using language. *arXiv preprint arXiv:2302.04269*, 2023. 2, 3
- [53] Zeliang Zhang, Mingqian Feng, Zhiheng Li, and Chenliang Xu. Discover and mitigate multiple biased subgroups in image classifiers. In *Proceedings of the IEEE/CVF Conference on Computer Vision and Pattern Recognition*, pages 10906–10915, 2024. 2
- [54] Jieyu Zhao, Tianlu Wang, Mark Yatskar, Vicente Ordonez, and Kai-Wei Chang. Men also like shopping: Reducing gender bias amplification using corpus-level constraints. *arXiv preprint arXiv:1707.09457*, 2017. 1

Common Sense Bias Modeling for Classification Tasks

Supplementary Material

7. Implementation

7.1. Augmentations

The image augmentations used in CSBD, which are implemented alongside the weighted sampling for bias mitigation, are also applied to the other methods for fair comparison. On CelebA we use the following augmentations:

- random resized cropping to 224×224 ;
 - horizontal flips;
 - color jitter;
- and on MS-COCO we use
- random resized cropping to 448×448 ;
 - horizontal flips;
 - RandAugment.

7.2. Training and Testing

The proposed CSBD bias modeling method is CPU-only and does not use any model training. For bias mitigation experiments on downstream tasks, the following training setups are consistent among comparison methods: We train all classification models for 100 epoches and select the best model on validation set to report its results on testing set. The classification model is ResNet50 [10]. SGD optimizer is used with learning rate of $1e^{-4}$, momentum of 0.9, and weight decay of 0.01. The batch size is set to be 256 on CelebA dataset and 32 on MS-COCO dataset. For all other method-specific hyper-parameters, we use the default values in the official repositories for LfF,⁵ DebiAN,⁶ and BPA,⁷ and for PGD we use the default values given in [1]. These experiments were developed using Pytorch and were performed on a Nvidia Tesla V100 GPU.

7.3. Algorithm

The detailed steps of CSBD method are provided in Algorithm 1.

8. Results - feature correlation list

We attach the full list of correlated common sense features discovered by our method, on CelebA dataset (Table 4), and MS-COCO dataset (Table 5 - Table 7) using dataset captions. It can be seen that many correlations are benign (that is, that the two features' co-occurrence is expected), which can only be judged from human knowledge. Therefore, we maintain a human-in-the-loop component to select spurious correlations from the lists to treat and mitigate downstream model bias.

Algorithm 1: CSBD. M is the size of the dataset. N is the total number of extracted noun phrase chunks. z is the distance threshold at or above which clusters will not be merged. F is the number of generated clusters or common sense features. β is the threshold of feature correlation coefficient.

Input: Image corpus $G = \{g_1, g_2, \dots, g_N\}$.

Description corpus $D = \{d_1, d_2, \dots, d_N\}$

Chunking and encoding:

$D \rightarrow P = \{p_1, p_2, \dots, p_N\}$

▷ P is the noun chunk set

$A = e(P) = \{\mathbf{p}_1, \mathbf{p}_2, \dots, \mathbf{p}_N\} \in \mathbb{R}^{N \times 512}$

▷ e is a pre-trained text embedding model

Agglomerative clustering:

$\{A, z\} \rightarrow \{C_1, \dots, C_F\}$, where $p_i \in C_j$

▷ C is a set of noun chunks whose embeddings are clustered together, viewed as a feature

Computing correlation:

for C_f from C_1 to C_F **do:**

$\mathbf{t}_f = \{t_1, t_2, \dots, t_M\}$, where $t_i = 1$, if

$\exists p \in C_f: p$ in d_i , else $t_i = 0$

▷ Binary presence indicator for feature C_f

for f from 1 to F **do:**

for f' from 1 to F , $f' \neq f$ **do:**

$\mathbf{t}_f, \mathbf{t}_{f'} \rightarrow \phi_{\mathbf{t}_f \mathbf{t}_{f'}}$ ▷ ϕ correlation coefficient

Outputs: $[C_f, C_{f'}, \phi_{\mathbf{t}_f \mathbf{t}_{f'}}]$, if $|\phi_{\mathbf{t}_f \mathbf{t}_{f'}}| > \beta$

⁵<https://github.com/alinelab/LfF/>

⁶<https://github.com/zhihengli-UR/DebiAN/>

⁷<https://github.com/skynbe/pseudo-attributes>

Feature 1	Feature 2	ϕ correlation coefficient
"thick/thin frame"	"eyeglasses"	0.1243
"thick/thin frame"	"no eyeglasses"	-0.1328
"eyeglasses"	"man"	0.0693
"eyeglasses"	"woman"	-0.0743
"no eyeglasses"	"man"	-0.0681
"no eyeglasses"	"woman"	0.0734
"forehead"	"eyeglasses"	0.0609
"forehead"	"a small portion"	0.3503
"the face"	"no eyeglasses"	-0.1849
"the face"	"eyeglasses"	0.1862
"the face"	"no smile"	0.0802
"the face"	"a smile"	-0.1012
"the face"	"happiness"	0.1261
"teeth visible"	"no smile"	-0.3348
"teeth visible"	"a smile"	0.2571
"mouth wide open"	"no smile"	-0.1826
"mouth wide open"	"happiness"	-0.0934
"mouth wide open"	"teeth visible"	0.1202
"a little bit open"	"the face"	-0.068
"forehead"	"man"	-0.0637
"forehead"	"woman"	0.0649
"no smile"	"happiness"	-0.2961
"no smile"	"teenager"	0.0506
"no smile"	"man"	0.1058
"a smile"	"man"	-0.0552
"man"	"the middle age"	0.0817
"man"	"medium length"	0.2204
"man"	"forties", "fifties"	0.0627
"beard"	"the middle age"	0.056
"mustache"	"the middle age"	0.0601
"beard"	"middle length"	0.18
"mustache"	"middle length"	0.1921
"beard"	"teenager"	-0.0504
"mustache"	"teenager"	-0.0527
"beard"	"no smile"	0.0754
"mustache"	"no smile"	0.0788
"beard"	"woman"	-0.3988
"mustache"	"woman"	-0.3939
"beard"	"man"	0.4498
"mustache"	"man"	0.4482

Table 4. The correlated feature pairs in CelebA dataset, reasoned by CSBD. Each feature is a cluster of descriptive phrases and only 1-2 representative phrases are shown in the table.

Feature 1	Feature 2	ϕ correlation coefficient
"soccer", "baseball"	"field"	0.1246
"baseball bat"	"field"	0.0902
"soccer", "baseball"	"the ball"	0.1638
"soccer", "baseball"	"a game"	0.149
"baseball bat"	"a ball"	0.1089
"soccer", "baseball"	"a man", "a boy"	0.0673
"sky", "air"	"a man", "a boy"	0.0558
"sky", "air"	"skateboard"	0.1252
"sky", "air"	"snowboard"	0.0903
"sky", "air"	"airplane"	0.0901
"sky", "air"	"kite"	0.1024
"men"	"a group"	0.085
"a man"	"a group"	-0.0666
"a man"	"frisbee"	0.0701
"a man"	"skateboard"	0.1263
"a man"	"snowboard"	0.0885
"men"	"two members"	0.0768
"men"	"two members"	0.0768
"a man"	"cellphone"	0.0523
"a man"	"hand", "fingers"	0.051
"a man"	"tennis racket"	0.0674
"a man"	"tennis player"	0.0758
"a man"	"umbrella"	0.062
"men"	"sneakers", "pants"	0.0621
"a man"	"wave"	0.0969
"a man"	"surfboard"	0.1102
"zebra"	"grass field"	0.1454
"giraffe"	"grass field"	0.1022
"zebra"	"sheep"	0.077
"zebra"	"trees"	0.0834
"giraffe"	"trees"	0.1644
"giraffe"	"fence"	0.0745
"a person"	"snowy slopes"	0.084
"a person"	"skateboard"	0.0635
"a person"	"snowboard"	0.0748
"bike"	"city street"	0.0675
"motorcycle"	"city street"	0.0504
"motorcycle"	"road"	0.0677
"bus"	"city street"	0.1364
"bus"	"road"	0.1072
"bathroom"	"vase"	0.1229
"sink"	"window"	0.085
"bathroom"	"window"	0.1092
"sink"	"toilet"	0.1667
"bathroom"	"toilet"	0.423
"snowy slopes"	"snowboard"	0.1701
"table"	"food"	0.1723
"table"	"pizza"	0.1123
"table"	"cake"	0.081
"table"	"beverages"	0.1173
"table"	"flower"	0.0642
"table"	"plate"	0.123
"table"	"bowl", "cup"	0.0697
"table"	"fresh produce"	0.0634
"table"	"vase"	0.079
"table"	"glasses"	0.0578
"food"	"kitchen"	0.0703
"food"	"plate"	0.2588
"food"	"a dish"	0.0693
"food"	"bowl", "cup"	0.0516
"food"	"egg", "sausage"	0.0545
"living room"	"game controller"	0.0574
"living room"	"pillow"	0.1643
"couch"	"dog"	0.058
"couch"	"cat"	0.0615

Table 5. The correlated feature pairs in MS-COCO dataset, reasoned by CSBD. Each feature is a cluster of descriptive phrases and only 1-2 representative phrases are shown in the table.

Feature 1	Feature 2	ϕ correlation coefficient
"the top", "the front"	"clock"	0.0594
"the top", "the front"	"car"	0.0543
"microwave", "oven"	"dishes"	0.0604
"kitchen"	"scissors"	0.0894
"a group"	"a game"	0.0588
"a group"	"people"	0.3927
"frisbee"	"field"	0.0616
"frisbee"	"a game"	0.0994
"frisbee"	"dog"	0.091
"plate"	"pizza"	0.1148
"plate"	"cake"	0.1013
"plate"	"sandwich"	0.2136
"plate"	"donuts"	0.0614
"plate"	"meat"	0.1573
"plate"	"vegetables"	0.1855
"plate"	"snacks"	0.1307
"plate"	"hot dogs"	0.0594
"plate"	"fruits"	0.074
"plate"	"beverages"	0.0627
"bowl", "cup"	"sandwich"	0.069
"bowl", "cup"	"beverages"	0.1497
"bowl", "cup"	"fruit"	0.1396
"bowl", "cup"	"vegetables"	0.1079
"bowl", "cup"	"bananas"	0.0625
"glasses"	"beverages"	0.136
"a pot"	"beverages"	0.0942
"a pot"	"flower"	0.2277
"sandwich"	"beverages"	0.0537
"sandwich"	"meat"	0.0725
"sandwich"	"vegetables"	0.0812
"hot dogs"	"vegetables"	0.1717
"donuts"	"beverages"	0.0515
"pizza"	"vegetables"	0.1046
"pizza"	"box"	0.0784
"cake"	"box"	0.1151
"donuts"	"box"	0.0664
"tray"	"pizza"	0.1309
"tray"	"cake"	0.0529
"tray"	"sandwich"	0.0586
"tray"	"vegetables"	0.105
"dish"	"vegetables"	0.0836
"skateboard"	"a line drive"	0.0849
"skateboard"	"boys"	0.1404
"grass field"	"cow"	0.1226
"grass field"	"sheep"	0.184
"grass field"	"elephant"	0.0516
"field"	"trees"	0.063
"sheep"	"birds"	0.0794
"bed"	"chairs"	0.051
"bedroom"	"chairs"	0.057
"bedroom"	"furniture"	0.0852
"bed"	"cat"	0.0609
"bags"	"a pack"	0.0506
"city"	"traffic lights"	0.0682
"cell phone"	"women"	0.0721
"desk"	"cat"	0.0753
"keyboard"	"cat"	0.1
"beach"	"kite"	0.1347
"beach"	"people"	0.0789
"beach"	"surfer"	0.1594
"beach"	"umbrella"	0.0768
"water", "ocean"	"boat"	0.1235
"water", "ocean"	"birds"	0.0558
"water", "ocean"	"shore"	0.1412
"water", "ocean"	"surfer"	0.2677

Table 6. The correlated feature pairs in MS-COCO dataset, reasoned by CSBD. Each "feature" is a cluster of descriptive noun chunks and only 1-2 representative noun chunks are shown in the table.

Feature 1	Feature 2	ϕ correlation coefficient
"a woman"	"tennis player"	0.0902
"a woman"	"umbrella"	0.0688
"city street"	"sign"	0.0743
"city street"	"traffic light"	0.1255
"fruit"	"a bunch"	0.0644
"bananas"	"a bunch"	0.0938
"clock"	"building"	0.1026
"airplane"	"airport"	0.1426
"trees"	"elephant"	0.0637
"a ball"	"tennis player"	0.1709
"a ball"	"tennis racket"	0.0833
"a ball"	"tennis court"	0.0827
"tennis court"	"a game"	0.0595
"a game"	"controllers"	0.1199
"a game"	"a man"	0.0642
"window"	"cat"	0.0574
"building"	"sign"	0.056
"a flattened area"	"train"	0.093
"boat"	"water flow"	0.0802
"fence"	"sign"	0.1064
"umbrella"	"people"	0.1001
"kite"	"people"	0.1023
"birds"	"water flow"	0.0522
"people"	"a crowd"	0.097

Table 7. The correlated feature pairs in MS-COCO dataset, reasoned by CSBD. Each "feature" is a cluster of descriptive noun chunks and only 1-2 representative noun chunks are shown in the table.